

# A QED Description of Quantum Coherence and Damping in Condensed Phase Energy Transfer

Jack. S. Ford<sup>1</sup>, A. Salam<sup>2-4,\*</sup> and Garth. A. Jones<sup>1,\*</sup>

1 School of Chemistry, University of East Anglia, Norwich, UK

2 Department of Chemistry, Wake Forest University, Winston-Salem, NC 27109, USA

3 Physikalische Institut, Albert-Ludwigs-Universität-Freiburg, Hermann-Herder-Strasse 3, D-79104, Freiburg, Germany

4 Freiburg Institut for Advanced Studies (FRIAS), Albertstrasse 19, D-79104, Freiburg, Germany

## Corresponding Authors

\* [salama@wfu.edu](mailto:salama@wfu.edu) \* [garth.jones@uea.ac.uk](mailto:garth.jones@uea.ac.uk)

ORCID: G. A. Jones: [0000-0003-2984-1711](https://orcid.org/0000-0003-2984-1711)

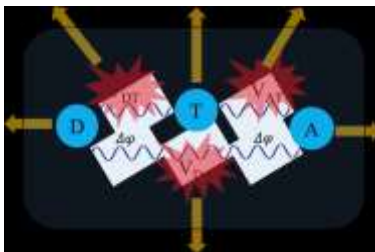
ORCID: A. Salam: [0000-0001-5167-4767](https://orcid.org/0000-0001-5167-4767)

## ABSTRACT:

Quantum coherence in condensed phase electronic resonance energy transfer (RET) is described within the context of quantum electrodynamics (QED) theory. Mediating dressed virtual photons (polaritons) are explicitly incorporated into the treatment and coherence is understood within the context of interfering Feynman pathways connecting the initial and final states for the RET

process. The model investigated is that of an oriented three-body donor, acceptor and mediator RET system embedded within a dispersive and absorbing polarizable medium. We show how quantum coherence can significantly enhance the rate of RET and give a rigorous picture for subsequent decoherence that is driven by both phase and amplitude damping. Energy conserving phase damping occurs as a result of geometric and dispersive effects and is associated with destructive interference between Feynman pathways. Dissipative amplitude damping, on the other hand, is attributed to vibronic relaxation and absorptivity of the medium and can be understood as virtual photons (polaritons) leaking into the environment. This model offers insights into the emergence of coherence and subsequent decoherence for energy transfer in photosynthetic systems.

## TOC GRAPHICS



**KEYWORDS** FRET, quantum biology, dissipative quantum systems, open quantum systems, quantum electrodynamics, quantum field theory

Quantum coherence is understood to be central to electronic resonance energy transfer (RET), the upstream process of biological photosynthesis,<sup>1-12</sup> although its exact nature is not without controversy.<sup>13-19</sup> It has been hypothesized that quantum coherence may enhance the efficiency of RET,<sup>20,21</sup> and it is also suggested that quantum coherence could be exploited as a valuable resource to improve the quality of quantum technologies.<sup>22</sup> Nevertheless, determining the exact nature and origin of coherence in condensed phase energy transfer is difficult. This is because

time-resolved two-dimensional optical experiments, typically used to investigate such phenomena, measure optical responses resulting from an induced macroscopic polarization, which is a classical property.<sup>23,24</sup> This is fundamentally different from many quantum optical experiments that investigate coherence, where the eigenvalues of relevant quantum mechanical operators, such as the spin polarization of photons, are measured directly,<sup>25</sup> or quantum non-demolition measurements are made.<sup>26</sup> Furthermore, many of the theoretical models used to simulate condensed phase RET are semi-classical in nature, assuming first-order, instantaneous, Coulombic interactions between chromophores.<sup>27</sup> In reality, RET is at least a second-order quantum dynamical process that is mediated by the exchange of virtual photons.<sup>28-33</sup> Consequently, it is extremely difficult to differentiate between classical and quantum mechanical origins of coherence; this has been highlighted previously.<sup>15</sup> Quantum mechanically, coherence is the superposition of wave functions in which phase relationships arise and persist for some time. In order to describe mixed states, this superposition of states is often written in terms of a density matrix. However, there is an alternative picture of coherence; namely, within a quantum dynamical setting it arises from the superposition of different Feynman pathways connecting a common initial state, with a common final state. This has been linked directly to the density matrix picture of coherence for a strongly driven optical system.<sup>34</sup>

In this work, an understanding of quantum coherence in RET is achieved at the level of interactions between fermions (valence electrons of the chromophores) via the exchange of bosons (mediating photons). This can only be achieved at the quantum field level, and the natural setting is through Feynman pathways, based on molecular QED.<sup>35-37</sup> While density matrix based open quantum system approaches do employ quantum mechanical equations of motion, and coherences can certainly emerge in the density matrix, the interactions (off-diagonal elements in the system Hamiltonian and system-bath interactions) do not generally incorporate mediating photons, and therefore the interactions are not derived from quantum mechanical principles. This time-independent approach focuses on quantum interactions, thereby providing microscopic details of coherence and decoherence in RET systems.

The relevant observable is the Fermi golden rule (FGR) rate,  $\Gamma = \frac{2\pi}{\hbar} |M_{fi}|^2 \rho_f$ , where  $\rho_f$  is the density of final states and  $M_{fi}$  is the (complex) quantum amplitude, often referred to as

the *probability amplitude*. We note that while the FGR is often associated with the classical rate through use of a classical coupling term, the present model employs the QED matrix element and consequently these coherences can only be purely quantum mechanical in nature – we invoke no semiclassical assumptions. Importantly, the RET processes we describe are directly analogous to quantum interference effects that, for example, arise from photons moving through a series of polarization filters or electrons moving through interference gates, both of which are prototypical examples of quantum coherence in application. We provide both analytical and numerical results describing how quantum coherence can enhance RET and how environmentally induced decoherence naturally occurs through damping. This work is carried out within the context of a third-body mediated RET process within an absorbing environment, which includes vibrational damping and both dispersion and absorption effects within a polarizable medium.

In RET, the transfer of a quantum of excitation energy between two chromophores arises from the exchange of a single virtual photon between donor (D) and acceptor (A). The mediating photon is by definition unobservable, being ‘borrowed’ from quantum fluctuations within the vacuum electromagnetic field, as permitted by the time-energy Heisenberg uncertainty relation.<sup>38</sup> The QED derived Fermi golden rule transfer rate for chromophores with fixed relative orientations in free space is,

$$\Gamma = \frac{\rho_f}{8\pi\epsilon_0^2\hbar} \rho^{-6} |\vec{\mu}^{0m}(D)|^2 |\vec{\mu}^{0m}(A)|^2 \left| \left( \eta_{ij}^{\vec{\rho}(3)} - ik_{m0}\rho\eta_{ij}^{\vec{\rho}(3)} - k_{m0}^2\rho^2\eta_{ij}^{\vec{\rho}(1)} \right) \hat{\mu}_i^D \hat{\mu}_j^A \right|^2, \quad (1)$$

where  $\vec{\rho} = \vec{R}_A - \vec{R}_D$  defines the distance between the donor and acceptor, which are positioned at  $\vec{R}_D$  and  $\vec{R}_A$ , respectively. These chromophores are by definition beyond significant wavefunction overlap. The transition electric dipole moments of  $\xi = D, A$  are  $\vec{\mu}^{0m}(\xi) = \langle 0_\xi | \vec{\mu}(\xi) | m_\xi \rangle$ , the wavenumber associated with the transition occurring in the emitter is  $k_{m0} = (E_m - E_0) / \hbar c$ , the number of levels per unit energy interval is defined through the density of states,  $\rho_f$  and the orientational factors are given by  $\eta_{ij}^{\vec{\rho}(t)} \square \delta_{ij} - t\hat{\rho}_i\hat{\rho}_j$  with  $t \in \{1, 3\}$ . Einstein summation convention is applied to repeating indices.

The familiar inverse sixth power dependence of the rate on inter-chromophore separation distance as predicted by Förster can be seen in Eq. (1). This is associated with short-range *radiationless* energy transfer. The inverse square (Coulombic) term is also evident, which is associated with the long-range *radiative* emission of a photon, with real character from D followed by its absorption by A. The middle term of the last factor dominates when the D-A distance is approximately equal to the reduced wavelength ( $\tilde{\lambda} = \lambda/2\pi$ ) of the exchanged photon. Collectively, this is known as the unified theory of RET.<sup>31,32,39-41</sup>

In a dielectric medium possessing a complex refractive index  $n$ , RET is mediated by a photon that is dressed by quantized electromagnetic fields of the bath called a *polariton*, instead of a free-space virtual photon, and the rate formula Eq. (1) is modified as described below. Contributions proportional to  $\rho^{-3}$  and  $\rho^{-5}$  appear in addition to  $\rho^{-x}$ ,  $x = 2, 4$  and  $6$ , and include explicit dependences on the real and imaginary parts of the refractive index ( $n$ ) of the medium, which account for dispersion and absorption, respectively. Consequently, screening and local field factors are also described in the rate formula as expected according to the Beer-Lambert Law, with the exponential decay factor scaling the transfer rate proportionally to the imaginary part of the refractive index. This underpins conventional macroscopic treatments of the environment.<sup>27,42-44</sup>

In this *Letter* we focus on how RET can be enhanced quantum mechanically and how damping and dissipation lead to environmentally induced decoherence. Our example is that of RET between a donor and acceptor in the presence of a polarisable third molecule, T, when all three chromophores are embedded in an absorbing medium. Of particular interest is how the rate of RET can be enhanced through interference effects between different Feynman pathways. This work complements a handful of papers in which a detailed molecular QED theory of third-body mediated RET occurring in free-space has been developed, and the relative importance of each contributing pathway has been delineated.<sup>45-48</sup> This recently developed formalism has already been applied to molecules, quantum dots, and nanowires.<sup>49-52</sup>

The RET matrix element involving the exchange of a polariton between D and A has an initial state with the donor initially in the  $m^{\text{th}}$  excited electronic state  $|m_D\rangle$  and the acceptor in the ground state  $|0_A\rangle$ . In our formulation we assume the donor and acceptor are chemically identical,

although this approximation can be easily relaxed without loss of generality. The initial state for the total system in which no polariton modes are occupied, is  $|i\rangle = |m_D, \mathbf{0}_A\rangle$ . The final state is where D is in its lowest level,  $|\mathbf{0}_D\rangle$ , and A is excited to state  $|m_A\rangle$ , with the polariton modes again remaining unoccupied, and is expressed as  $|f\rangle = |\mathbf{0}_D, m_A\rangle$ .

Within the context of a perturbation theory solution, the coupling between matter and quantized electromagnetic radiation is given by the electric dipole approximated form of the interaction Hamiltonian,<sup>35,36</sup>

$$H_{int}(\xi) = -\varepsilon_0^{-1} \vec{\mu}(\xi) \cdot \vec{d}^\perp(\vec{R}_\xi), \quad (2)$$

where  $\vec{\mu}(\xi)$  is the electric dipole moment operator of species  $\xi$ . The quantized field is expressed as a Fourier series mode expansion for the transverse electric displacement field operator. In vacuum form it is given by

$$\vec{d}^\perp(\vec{r}) = i \sum_{\vec{k}, \lambda} \frac{\hbar c k \varepsilon_0}{2V} \left[ \vec{e}^{(\lambda)}(\vec{k}) a^{(\lambda)}(\vec{k}) e^{i\vec{k}\cdot\vec{r}} - \vec{e}^{(\lambda)}(\vec{k}) a^{\dagger(\lambda)}(\vec{k}) e^{-i\vec{k}\cdot\vec{r}} \right], \quad (3)$$

where the sum is taken over all radiation field modes with  $\vec{k}$  the wave vector and  $\lambda$  the polarisation index for light in a box of volume  $V$ , with circular frequency  $\omega = ck$ . The operators  $a^{(\lambda)}(\vec{k})$  and  $a^{\dagger(\lambda)}(\vec{k})$ , destroy and create a photon respectively, with the number operator defined as  $a^{\dagger(\lambda)}(\vec{k}) a^{(\lambda)}(\vec{k})$  denoting the number of light quanta in the radiation field. These individual boson operators satisfy the following commutator relationship involving these two operators,<sup>53</sup>

$$[a^{(\lambda)}(\vec{k}), a^{\dagger(\lambda)}(\vec{k}')] = (8\pi^3 V)^{-1} \delta^3(\vec{k} - \vec{k}') \delta_{\lambda\lambda'}, \quad (4)$$

where  $\delta^3(\vec{k} - \vec{k}')$  is a Dirac delta function and  $\delta_{\lambda\lambda'}$  is a Kronecker delta, with all other operator combinations commuting.

In a dielectric medium, the mode expansion for the electric displacement field needs to be modified to,<sup>54-56</sup>

$$\vec{d}^{\perp(med)}(\vec{r}) = i \frac{\hbar \omega_p v_g^{(\nu)} \epsilon_0}{2cn^{(\nu)}V} \frac{(n^{(\nu)})^2 + 2}{3} \vec{e}^{(\eta)}(\vec{p}) P_\nu^{(\eta)}(\vec{p}) e^{i\vec{p}\cdot\vec{r}} - \vec{e}^{(\eta)}(\vec{p}) P_\nu^{\dagger(\eta)}(\vec{p}) e^{-i\vec{p}\cdot\vec{r}} \quad (5)$$

where the mode of the polariton is defined by its momentum and polarization,  $\vec{p}, \eta$ ;  $\nu$  is an index that specifies the polariton dispersion branch, in which  $v_g^{(\nu)}$  is the group velocity of radiation propagating in the medium whose refractive index is  $n^{(\nu)}$ ;  $P_\nu^{(\eta)}(\vec{p})$  and  $P_\nu^{\dagger(\eta)}(\vec{p})$  are the counterparts to  $a^{(\lambda)}(\vec{k})$  and  $a^{\dagger(\lambda)}(\vec{k})$ , respectively. See SI for more details on the theory of RET in condensed phase media.

In the case of *direct* RET between D and A,<sup>54</sup> two time-ordered Feynman diagrams contribute to the matrix element; one of these is shown in Figure 1(a). Each diagram depicts the exchange of a single virtual polariton between donor and acceptor. Using second-order time-dependent perturbation theory for the probability amplitude, the matrix element is derived as;

$$M_{fi}^{DA(med)} = \mu_i^{0m}(D) V_{ij}^{(med)}(k_{m0}, \vec{p}) \mu_j^{m0}(A), \quad (6)$$

where the Einstein summation convention has been adopted; repeating indices of Cartesian tensor components, denoted by Latin subscripts in the space-fixed frame of reference, being summed. The other quantity appearing in Eq. (6) is the tensor coupling the two dipoles in a medium, which takes the form<sup>54</sup>

$$V_{ij}^{(med)}(p, \vec{r}) = n^{-2} \frac{n^2 + 2}{3} V_{ij}^{(vac)}(np, \vec{r}), \quad (7)$$

where  $n$  is the complex refractive index of the medium in which the molecules are embedded, and  $V_{ij}^{(vac)}(np, \vec{r})$  is the vacuum form of the retarded electric dipole-electric dipole interaction tensor,<sup>35,36</sup> whose wave vector argument is scaled by  $n$ ,

$$\begin{aligned}
V_{ij}^{(vac)}(p, \vec{r}) &= -\frac{1}{4\pi\epsilon_0} \left( -\nabla^2 \delta_{ij} + \nabla_i \nabla_j \right) \frac{e^{ipr}}{r} \\
&= \frac{e^{ipr}}{4\pi\epsilon_0 r^3} \left[ (\delta_{ij} - 3\hat{r}_i \hat{r}_j)(1 - ipr) - (\delta_{ij} - \hat{r}_i \hat{r}_j) p^2 r^2 \right].
\end{aligned} \tag{8}$$

For the current application,  $p \in \{0, k_{m0}\}$ .

In the weak coupling regime within a medium the rate becomes,

$$\begin{aligned}
\Gamma^{DA(med)} &= \frac{\rho_f}{8\pi\epsilon_0^2 \hbar} \frac{n^2 + 2}{3n} e^{-2\text{Im}(n)k_{m0}\rho} \rho^{-6} \left| \vec{\mu}^{0m}(D) \right|^2 \left| \vec{\mu}^{0m}(A) \right|^2 \\
&\quad \times \left| \left( \eta_{ij}^{\tilde{\rho}(3)} - ink_{m0}\rho \eta_{ij}^{\tilde{\rho}(3)} - n^2 k_{m0}^2 \rho^2 \eta_{ij}^{\tilde{\rho}(1)} \right) \hat{\mu}_i^D \hat{\mu}_j^A \right|^2,
\end{aligned} \tag{9}$$

in contrast to the free-space result given by Eq. (1). As previously, we use the shorthand notation  $\eta_{ij}^{\tilde{\rho}(t)} \equiv \delta_{ij} - t\hat{\rho}_i \hat{\rho}_j$ ,  $t \in \{1, 3\}$  for the orientational factors. Screening and local field effects are accounted for through the pre-factors that depend upon  $n$ , as are dissipative effects in the medium which are introduced through the exponential factor, whose argument displays a negative dependence on the imaginary part of  $n$  due to the identity  $|e^{iz}|^2 = e^{-2\text{Im}(z)}$ . Eq. (9) reduces naturally to its free-space form on choosing  $\text{Re}(n) = 1$  and  $\text{Im}(n) = 0$ .

Now let us consider how the mechanism changes upon the introduction of the third species (T) that is assumed to be neutral and passive, residing in the ground electronic state at initial and final times. Indirect as well as direct migrations of energy between D and A can now occur. That is to say, the transfer is now *mediated*. In total, there are four possible coupling configurations that facilitate the overall RET process, considering mechanisms up to fourth order in perturbation theory, as shown in Figure 1. Namely, direct transfer from D to A, and three pathways involving the mediator T: the bridging mechanism DTA in which T relays the energy it receives from D onto A, and two situations in which T is coupled only to the donor or only to the acceptor, designated as the TDA and DAT mechanisms, respectively (other mechanisms do exist, but at higher levels of perturbation theory, which have minimal effect). In these last two cases it is necessary for T to be polar, possessing a ground state permanent electric dipole moment,  $\vec{\mu}^{00}(T)$ . That is, no net



transfer of energy occurs between T and D in the TDA mechanism, or between A and T in the DAT pathway. Figure 1 shows one Feynman diagram for each of the four RET scenarios. However, it must be noted that when calculating the rate of RET, all time orderings of light-matter interaction should be included, giving a total of 74 Feynman diagrams ( $2! = 2$  for the direct case, and  $4! = 24$  for each of the third-body mediated pathways).

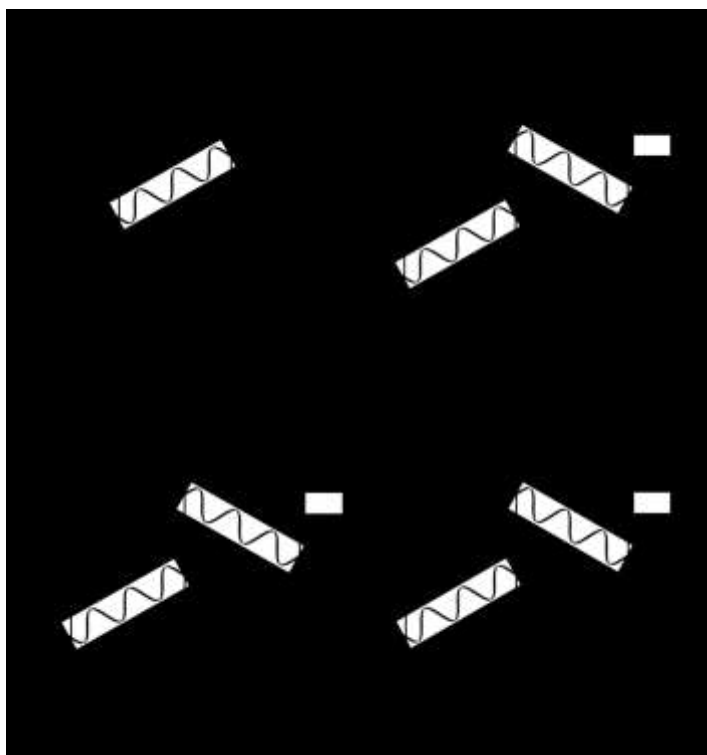


**Figure 1.** Example Feynman diagrams for direct RET and the three mediated mechanisms. Time moves upwards, straight lines represent molecular states, and wavy lines polariton states. (a) DA configuration (direct donor-acceptor coupling). (b) TDA configuration (third molecule couples to donor). (c) DAT configuration (third molecule couples to acceptor), and (d) DTA configuration (donor and acceptor each couple to a third mediating molecule). There are 2 pathways for (a) and 24 for (b) – (d), making a total of 74 diagrams.

How does the third-body, T, modify the rate of RET between D and A in a medium with complex refractive index  $n$ ? In our model system, we assume that each species has a specified position and relative orientation with respect to the other two chromophores. Such a situation is pertinent when investigating quantum coherence effects in supramolecular complexes such as antenna structures in light-harvesting systems.

Each of the contributions to the rate dependent upon T must be evaluated using fourth-order time-dependent perturbation theory (i.e. there are four linear in the electric displacement field light-matter interactions involved). Furthermore, we must include all time-ordered diagrams at each contributing order of perturbation theory in the calculation. A single virtual photon propagates between each pair of coupled particles so that twenty-four Feynman diagrams contribute to each of the three pathways involving the mediator, and the two for the direct transfer process, as depicted in Figure 1. Since species T remains unchanged in its ground electronic state  $|0_T\rangle$  prior to and after the excitation transfer events, the total system initial and final states given before Eq. (2) are easily modified to account for the presence of the third-body, which may, incidentally, undergo virtual electronic transitions to an arbitrary state  $|r_T\rangle$  during the intermediate (in-process) time period. This requires that A's final state is  $|m_A\rangle$  and that the transfer is resonant. In the case considered here, where the three chromophores are chemically identical, electric dipole moments and polarisabilities for the three species have equal magnitudes for their expectation values taken over the same electronic state, and similarly for other observable quantities.

As a consequence of the distinct possible pathways, the total probability amplitude connecting the initial and final states consists of four terms:

$$M_{fi}^{Total} = M^{DA} + M^{TDA} + M^{DAT} + M^{DTA}. \quad (10)$$

The first term of Eq. (10) is given by Eq. (6). Explicit expressions for the individual contributions to the total matrix element Eq. (10) that depend on T are evaluated using standard methods of molecular QED theory.<sup>35,36</sup> They are:

$$M^{TDA} = \mu_i^{00}(T) V_{ij}^{med}(0, \vec{R}) \alpha_{jk}^{0m}(D; -k, 0) V_{kl}^{med}(k, \vec{\rho}) \mu_l^{m0}(A), \quad (11)$$

$$M^{DAT} = \mu_i^{0m}(D) V_{ij}^{med}(k, \vec{\rho}) \alpha_{jk}^{m0}(A; 0, k) V_{kl}^{med}(0, \vec{R}') \mu_l^{00}(T), \quad (12)$$

and

$$M^{DTA} = \mu_i^{0m}(D) V_{ij}^{med}(k, \vec{R}) \alpha_{jk}^{00}(T; -k, k) V_{kl}^{med}(k, \vec{R}') \mu_l^{m0}(A). \quad (13)$$

The effect of the medium is included through the coupling tensor Eq. (7). The relative displacement vectors are defined as  $\vec{R} = \vec{R}_D - \vec{R}_T$ , and  $\vec{R}' = \vec{R}_A - \vec{R}_T$ , so that  $\vec{\rho} = \vec{R}' - \vec{R}$  is consistent with its definition given earlier. The site at which a virtual photon is scattered features in the amplitude via its polarisability tensor: a transition polarisability is required in the case of the TDA and DAT mechanisms, and the ground state counterpart for T in the case of the DTA pathway. For any two-photon allowed molecular process occurring between states  $|i\rangle$  and  $|f\rangle$ , the general form of the frequency dependent transition polarisability of particle  $\xi$  is given by

$$\alpha_{ij}^{fi}(\xi; -p', p) = \sum_r \frac{\mu_i^{fr}(\xi)\mu_j^{ri}(\xi)}{E_{ir} + \hbar cp + i\hbar c\gamma^{(r)}} + \frac{\mu_j^{fr}(\xi)\mu_i^{ri}(\xi)}{E_{ir} - \hbar cp' + i\hbar c\gamma^{(r)}}, \quad (14)$$

where the sum is over all intermediate levels  $|r_\xi\rangle$ , and the damping of the molecule in this state is denoted by  $\gamma^{(r)}$ . The reciprocal length appearing in the arguments of the coupling tensor and polarisability correspond to the amount of transferred energy,  $E_{m0} = E_m - E_0 = \hbar ck_{m0}$ , with  $k_{m0} = k$  chosen for notational convenience. The three relevant polarisabilities are:

$$\alpha_{ij}^{0m}(D; -k, 0) = \frac{\mu_i^{00}(D)\mu_j^{0m}(D)}{E_{m0} + i\hbar c\gamma^{(0)}} + \frac{\mu_j^{00}(D)\mu_i^{0m}(D)}{i\hbar c\gamma^{(0)}} + \frac{\mu_i^{0m}(D)\mu_j^{mm}(D)}{i\hbar c\gamma^{(m)}} + \frac{\mu_j^{0m}(D)\mu_i^{mm}(D)}{-E_{m0} + i\hbar c\gamma^{(m)}}, \quad (15a)$$

$$\alpha_{ij}^{m0}(A; 0, k) = \frac{\mu_i^{m0}(A)\mu_j^{00}(A)}{E_{m0} + i\hbar c\gamma^{(0)}} + \frac{\mu_j^{m0}(A)\mu_i^{00}(A)}{i\hbar c\gamma^{(0)}} + \frac{\mu_i^{mm}(A)\mu_j^{m0}(A)}{i\hbar c\gamma^{(m)}} + \frac{\mu_j^{mm}(A)\mu_i^{m0}(A)}{-E_{m0} + i\hbar c\gamma^{(m)}}, \quad (15b)$$

$$\alpha_{ij}^{00}(T; -k, k) = \frac{\mu_i^{00}(T)\mu_j^{00}(T)}{E_{m0} + i\hbar c\gamma^{(0)}} + \frac{\mu_j^{00}(T)\mu_i^{00}(T)}{-E_{m0} + i\hbar c\gamma^{(0)}} + \frac{\mu_i^{0m}(T)\mu_j^{m0}(T)}{i\hbar c\gamma^{(m)}} + \frac{\mu_j^{0m}(T)\mu_i^{m0}(T)}{-2E_{m0} + i\hbar c\gamma^{(m)}}. \quad (15c)$$

In the case of the TDA and DAT mechanisms, no net energy is relayed by T. Consequently, coupling of T is through its ground state permanent electric dipole moment, so the wave number argument appearing in  $V_{ij}^{med}$  and the polarisability is zero in Eqs. (11) and (12), corresponding to the static or zero-frequency forms of these two quantities. The five relevant coupling tensors present in the matrix elements (11) – (13) are:

$$V_{ij}^{med}(0, \vec{R}) = \frac{1}{4\pi\epsilon_0 R^3} \frac{n^2 + 2}{3n} \eta_{ij}^{\vec{R}(3)}, \quad (16)$$

$$V_{ij}^{med}(k, \vec{\rho}) = \frac{1}{4\pi\epsilon_0 \rho^3} \frac{n^2 + 2}{3n} e^{ink\rho} \eta_{ij}^{\vec{\rho}(3)} - ink\rho \eta_{ij}^{\vec{\rho}(3)} - n^2 k^2 \rho^2 \eta_{ij}^{\vec{\rho}(1)}, \quad (17)$$

$$V_{ij}^{med}(0, \vec{R}') = \frac{1}{4\pi\epsilon_0 R'^3} \frac{n^2 + 2}{3n} \eta_{ij}^{\vec{R}'(3)}, \quad (18)$$

$$V_{ij}^{med}(k, \vec{R}) = \frac{1}{4\pi\epsilon_0 R^3} \frac{n^2 + 2}{3n} e^{inkR} \eta_{ij}^{\vec{R}(3)} - inkR \eta_{ij}^{\vec{R}(3)} - n^2 k^2 R^2 \eta_{ij}^{\vec{R}(1)}, \quad (19)$$

$$V_{ij}^{med}(k, \vec{R}') = \frac{1}{4\pi\epsilon_0 R'^3} \frac{n^2 + 2}{3n} e^{inkR'} \eta_{ij}^{\vec{R}'(3)} - inkR' \eta_{ij}^{\vec{R}'(3)} - n^2 k^2 R'^2 \eta_{ij}^{\vec{R}'(1)}. \quad (20)$$

Substituting the total matrix element Eq. (10) into the Fermi golden rule rate formula produces ten contributory terms according to the complex identity:

$$\begin{aligned} \Gamma^{Total} &= \frac{2\pi\rho_f}{\hbar} \left[ |M^{DA}|^2 \right. \\ &+ 2\text{Re}\left(M^{DA} \bar{M}^{TDA}\right) + |M^{TDA}|^2 \\ &+ 2\text{Re}\left(M^{DA} \bar{M}^{DAT}\right) + 2\text{Re}\left(M^{TDA} \bar{M}^{DAT}\right) + |M^{DAT}|^2 \\ &+ 2\text{Re}\left(M^{DA} \bar{M}^{DTA}\right) + 2\text{Re}\left(M^{TDA} \bar{M}^{DTA}\right) + 2\text{Re}\left(M^{DAT} \bar{M}^{DTA}\right) + |M^{DTA}|^2 \left. \right] \end{aligned} \quad (21)$$

The individual terms within the rate equation can be broken down into pure terms (red), cross-terms involving the direct and indirect mechanisms (blue) and the cross-terms for different indirect mechanisms (magenta). The pure terms are all positive terms containing amplitudes only and must therefore enhance the rate of RET. The cross-terms are interferences between matrix elements. In order to appreciate the nature of these terms, Eq. (21) can be rewritten with phase factors for each possible transfer pathway included explicitly, with that associated with the direct mechanism denoted by  $\varphi_{DA}$ . Similar notations are used for the other migration routes. This will enable the

dependence of the RET rate on the phase of the amplitude associated with each term in Eq. (21) to be readily accounted for, as seen in Eq. (22).

$$\begin{aligned}
& \left| |M^{DA}| \exp(i\varphi_{DA}) + |M^{TDA}| \exp(i\varphi_{TDA}) + |M^{DAT}| \exp(i\varphi_{DAT}) + |M^{DTA}| \exp(i\varphi_{DTA}) \right|^2 \\
&= \left[ |M^{DA}|^2 \right. \\
&+ 2|M^{DA}M^{TDA}| \cos(\varphi_{DA} - \varphi_{TDA}) + |M^{TDA}|^2 \\
&+ 2|M^{DA}M^{DAT}| \cos(\varphi_{DA} - \varphi_{DAT}) + 2|M^{TDA}M^{DAT}| \cos(\varphi_{TDA} - \varphi_{DAT}) + |M^{DAT}|^2 \\
&+ 2|M^{DA}M^{DTA}| \cos(\varphi_{DA} - \varphi_{DTA}) + 2|M^{TDA}M^{DTA}| \cos(\varphi_{TDA} - \varphi_{DTA}) + 2|M^{DAT}M^{DTA}| \cos(\varphi_{DAT} - \varphi_{DTA}) + |M^{DTA}|^2 \left. \right]
\end{aligned} \tag{22}$$

Eq. (22) shows clearly how the presence of the mediator, T, can influence the rate of RET through quantum coherence. Notably, the phase differences indicate that the cosine terms must lie between +1 and -1, and consequently either constructive or destructive interference may occur for the a particular pathway. It is notable that a key parameter in the phase terms is the location of the chromophores with respect to each other, through Eqs. (17), (19) and (20). However, the existence of other imaginary terms including the damping term in the polarisability tensors, Eqs. (15), means that quantum phase relationships in RET systems are very complicated, emphasizing the subtlety of quantum coherence - even for a simple 3-body model system.

Both amplitude damping and phase damping are phenomena well known with theories of *Quantum Noise*.<sup>57,58</sup> Now we consider the role of these types of damping and how they give rise to decoherence in condensed phase RET systems, at the microscopic level. This is achieved with the help of numerical simulations that show quantitatively how RET can be enhanced through quantum coherence consisting of both phase and amplitude contributions seen in Eq. (22). Furthermore, we consider how damping and absorption by the medium will destroy these coherences. We consider a model donor, acceptor and mediator system which is linear lying along the  $z$ -axis, with  $R_{DT} = R_{TA} = 0.7$  nm (1.4 nm separating the donor and acceptor). The transition dipole moment (TDM) for D is aligned along the  $x$ -axis and that of A is aligned at  $x = y$ . The magnitude of the transition energies is taken to be  $6.32 \times 10^{-19}$  J and the TDM magnitudes are 3.33

$\times 10^{-29}$  C m. The reported relative rates are normalized to the rate of direct RET between the donor and acceptor only, as shown by Eq. (9).

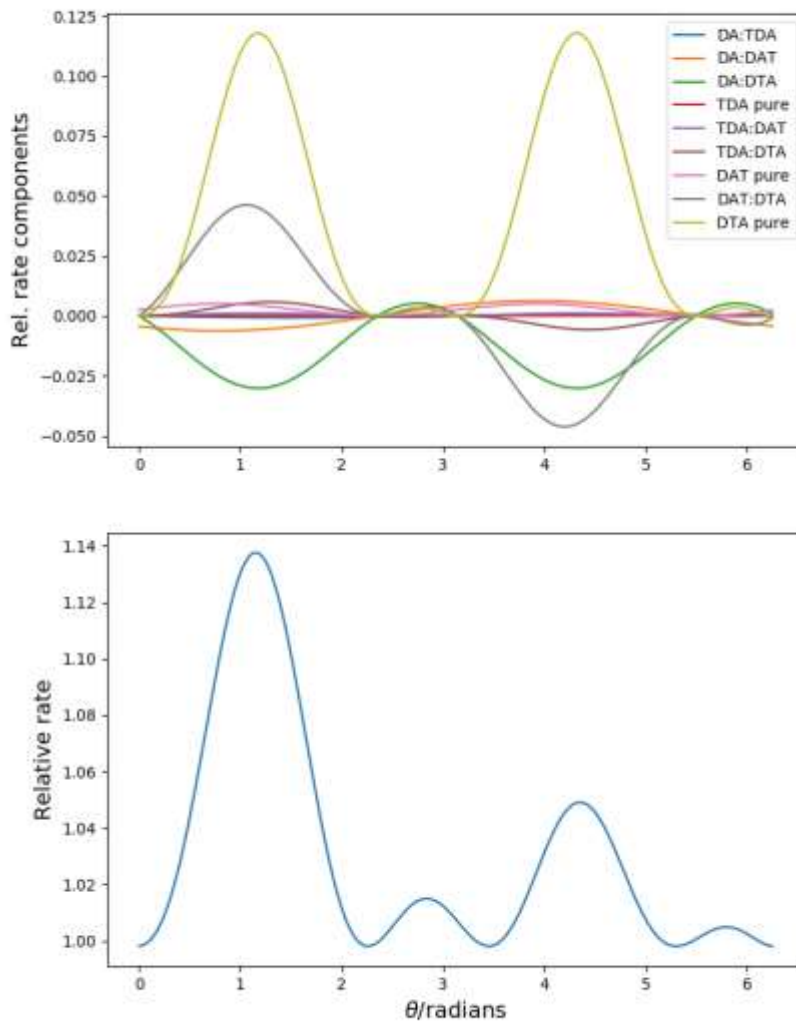


**Figure 2:** (Upper) Shows the magnitude of the individual components of the relative rate in Eqs. (21) and (22). These are normalized to the direct term  $|M^{DA}|^2 = 1$ . (Lower) Shows the rate relative to direct RET, with the global maximum at 1.16 radians for the model system.

In the first set of simulations, Figure 2, the TDM of T is in the  $x$ - $y$  plane and is rotated about the  $z$ -axis ( $\Theta$ ), starting parallel with the positive  $x$ -axis. Figure 2 (upper) shows how the individual contributions to the probability amplitude in Eqs. (21) and (22), vary as a function of  $\Theta$ . Figure 2 (lower) shows the total probability, indicating some specific geometries where quantum coherence strongly enhances the rate, with the global maximum at  $\Theta = 1.16$  radians. As might be expected, the major positive contribution to the rate is from  $|M^{DTA}|^2$ , the pure-term involving T as a mediator. Interestingly, there are two important cross-terms, both involving DTA,  $2\text{Re}(M^{DAT}\bar{M}^{DTA})$  and  $2\text{Re}(M^{DA}\bar{M}^{DTA})$  which involve both amplitude and phase effects and can reduce as well as enhance the rate of RET.

We now consider how damping can lead to quantum decoherence, dramatically reducing the rate of energy transfer, until it approaches the direct rate. Here we set to a static system geometry, with the angle of rotation of T equal to 1.16 radians, to coincide with the maximum transfer rate seen in Figure 2. Figure 3 shows the result of increasing the vibronic damping parameter  $\gamma^{(r)}$ . Here we can see that increasing the damping results in rapid loss of coherence, with the pure rate term,  $|M^{DTA}|^2$  falling away more quickly than the interference terms containing phases,  $2\text{Re}(M^{DAT}\bar{M}^{DTA})$  and  $2\text{Re}(M^{DA}\bar{M}^{DTA})$ . It is notable that terms involving  $M^{TDA}$  and  $M^{DAT}$  are small and static. This is because there is no exchange of energy between D and T or T and A in those cases.

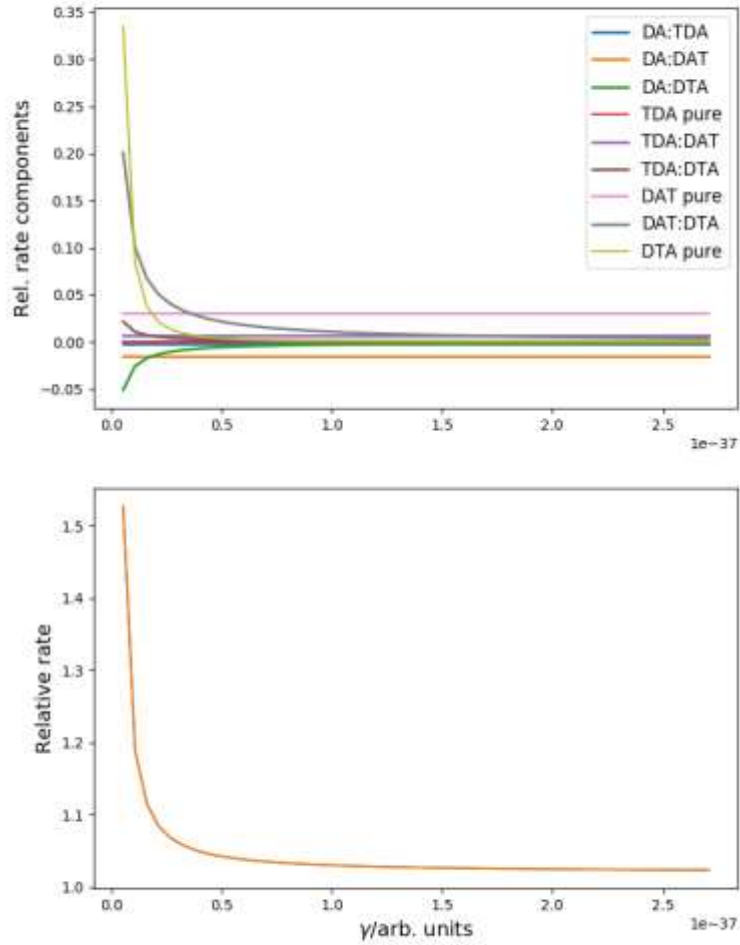


**Figure 3.** Increasing the damping parameter,  $\gamma^{(r)}$ . (Upper) The rate components and (lower) the total rate, normalized to  $|M^{DA}|^2 = 1$ .

Figure 4 shows how the refractive index affects the magnitude of the rate components leading to a reduction in the rate of RET for the ranges considered. The upper figure showing the dependence on  $\text{Re}(n)$  and the lower showing  $\text{Im}(n)$ . It can be seen that both dispersion and absorption also give rise to a reduction in the probability for RET, although the dependencies are much more gentle.



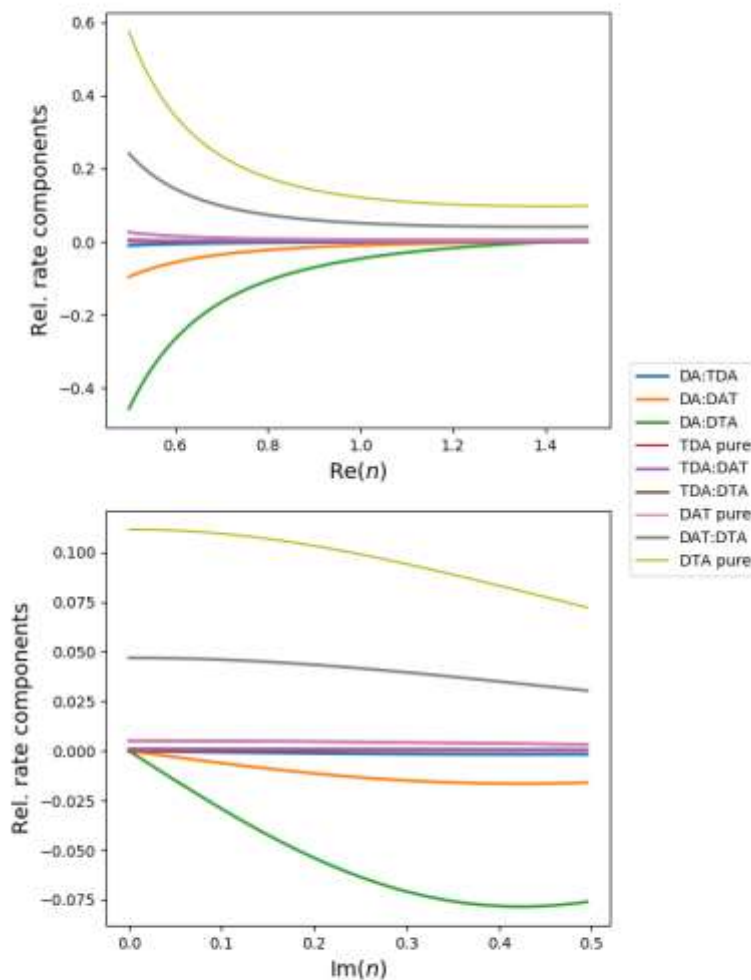


**Figure 4.** Rate components as a function of changing refractive index, normalized to  $|M^{DA}|^2 = 1$ . (Upper) Real part of the refractive index representing dispersion, (lower) Imaginary part of the refractive index representing absorption.

It is well known that the rate of RET is strongly dependent on the distances between the chromophores and relative orientations between the electronic transition dipole moments. This is understood within classical Förster theory. However in mediated RET, we can see that quantum

coherence involving T can enhance RET through phases of the electromagnetic coupling tensors involving  $\vec{R}$  and  $\vec{R}'$  in Eqs. (19) and (20), as demonstrated in Figure 2. In fact, these interference terms can give rise to finite RET rates where it is formally forbidden for the pure DA system.

In the absence of damping, the predicted rate of third-body-mediated RET tends to infinity due to infinite polarisability; this is the singularity of perfect resonance. The damping in the polarisability,  $\gamma^{(r)}$ , may be physically attributed to vibronic coupling (although quantitative parameterization of an imaginary infinitesimal quantity would be challenging). This is to say, while residing in some specific electronic state  $r$ , a molecule is able to exchange energy with its mechanical degrees of freedom and ultimately an external bath. However, little work has been done on the development of open quantum field theories,<sup>59</sup> and hence these energy transactions are not accounted for explicitly in the time-independent closed-system formulation used here. The damping  $\gamma^{(r)}$  appears as a phenomenological parameter in Eq. (15), and hence denominators of the polarisability tensor terms describe the differences in total system energy between different regions of the Feynman diagrams. Introducing an imaginary part to this energy scale represents non-Hermiticity in the total Hamiltonian operator describing the system, which accounts for dissipation.<sup>60</sup> Non-Hermiticity of Eq. (2) breaks overall time-symmetry, and Noether’s theorem suggests that time-asymmetry is equivalent to the system failing to satisfy overall conservation of energy. Therefore, inclusion of damping renders the overall system effectively “open”.

The real part of the refractive index  $\text{Re}(n)$  gives rise to an additional phase in Eqs. (17), (19) and (20) because the total refractive index is multiplied by  $i$ . This introduces a phase off-set that can be considered as a scattering event, leading to energy conserving phase damping. On the other hand, the imaginary part of the refractive index  $\text{Im}(n)$  may be interpreted as the overall opacity or absorptivity of the medium in which the three molecules are embedded. This is analogous to the mediating polaritons being absorbed by additional solvent molecules surrounding the RET complex. Similar to vibronic damping, the imaginary part describes the deviation from a perfectly energy-conserving closed system, allowing for irreversible energy loss. The distance-dependent decay factors  $e^{-2\text{Im}(n)k\rho}$  and  $e^{-2\text{Im}(n)k(R+R')}$  in Eqs. (17), (19) and (20) recreate the Beer-Lambert absorption law.

There are consequently several forms of damping that describe quantum channels for the decay of the system state  $|i\rangle$ , in addition to (and competing with) the RET process that results in  $|f\rangle$ . For a static molecular geometry, vibronic damping,  $\gamma^{(r)}$  occurs at each molecule, while dispersive and absorptive effects occur at each coupling; these act to diminish the probability of each system in state  $|i\rangle$  successfully arriving at state  $|f\rangle$ . The processes involved are complicated but there are clear manifestations of both amplitude damping and phase damping. Amplitude damping, at the quantum field level, can be thought of as virtual photons leaking from the system, meaning they are unable to access the final state to complete the RET process, thereby reducing the overall rate of RET. Phase damping on the other hand is an energy conserving process that affects only the blue and magenta cross-terms in the rate equation, which are essentially quantum interference terms traditionally associated with coherences.

As Scholes recently highlighted,<sup>61</sup> coherence is a universal phenomenon seen throughout nature, and there is much debate in the literature over the origin of coherences arising in RET of photosynthetic systems; whether excitonic or vibronic in nature, whether it should be defined as classical or quantum.<sup>15</sup> When addressing the role of quantum coherence, it is also important to recognize that coherence is dependent on the quantum mechanical basis used.<sup>22</sup> This work gives insights into the nature of quantum coherence in RET systems, namely how pure-terms enhance the rate of RET while the cross-terms can give rise to destructive as well as constructive interference. It has been alluded to that nature may exploit the geometry of supramolecular antenna systems to optimize RET processes,<sup>3,8</sup> and while that question is outside the scope of this theoretical work, the model we present certainly supports the possibility. Furthermore we provide detailed damping mechanisms that lead to decoherence. We emphasize that because this work is done within a gauge-invariant closed quantum system framework, while we have provided a rigorous microscopic mechanism with which decoherence occurs within an RET system, estimating rates of decoherence in RET systems is outside the scope of the present study. More work needs to be done to achieve this because of the lack of time-dependent quantum field theories that are gauge-invariant.<sup>37</sup>

## ACKNOWLEDGMENT

Part of the research presented in this paper was carried out on the High Performance Computing Cluster supported by the Research and Specialist Computing service at the University of East Anglia. AS acknowledges the award of a Mercator Fellowship funded by the Deutsche Forschungsgemeinschaft through the IRTG 2079/Cold Controlled Ensembles in Physics and Chemistry at the University of Freiburg. He also thanks the Freiburg Institute for Advanced Studies (FRIAS), University of Freiburg for the award of a Marie S Curie External Senior Fellowship under the EU Horizon 2020 Grant No. 75430.

## REFERENCES

1. Engel, G.S.; Calhoun, T.R.; Read, E.L.; Ahn, T.-K.; Mančal, T.; Cheng, Y.-C.; Blankenship, R.E.; Fleming, G.R. Evidence for wavelike energy transfer through quantum coherence in photosynthetic systems. *Nature*, **2007**, *446*, 782 – 786.
2. Collini, E.; Wong, C.Y.; Wilk, K.E.; Curmi, P.M.G.; Brumer, P.; Scholes, G.D. Coherently wired light-harvesting in photosynthetic marine algae at ambient temperature. *Nature*, **2010**, *463*, 644 – 647.
3. Scholes, G.D.; Fleming, G.R.; Olaya-Castro, A.; van Grondelle, R. Lessons from nature about solar light harvesting. *Nature Chem.*, **2011**, *3*, 763 – 774.
4. Panitchayangkoon, G.; Hayes, D.; Fransted, K.A.; Caram, J.R.; Harel, E.; Wen, J.; Blankenship, R.E.; Engel, G.S. Long-lived quantum coherence in photosynthetic complexes at physiological temperature. *Proc. Natl. Acad. Sci. U. S. A.*, **2010**, *107*, 12766 – 12770.
5. Fuller, F.D.; Pan, J.; Gelzinis, A.; Butkus, V.; Senlik, S.S.; Wilcox, D.E.; Yocum, C.F.; Valkunas, L.; Abramavicius, D.; Ogilvie, J.P. Vibronic coherence in oxygenic photosynthesis. *Nature Chem.* **2014**, *6*, 706 – 711.
6. Hildner, R.; Brinks, D.; Nieder, J.B.; Cogdell, R.J.; van Hulst, N.F. Quantum coherent energy transfer over varying pathways in single light-harvesting complexes. *Science*, **2013**, *340*, 1448 – 1451.

7. Chenu, A.; Scholes, G.D. Coherence in energy transfer and photosynthesis. *Ann. Rev. Phys. Chem.*, **2015**, *66*, 69 – 96.
8. Scholes, G.D. Quantum-coherent electronic energy transfer: Did nature think of it first?. *J. Phys. Chem. Lett.* **2010**, *1*, 2 – 8.
9. Ishizaki, A.; Fleming, G.R. Quantum coherence in photosynthetic light harvesting. *Ann. Rev. Condens. Matter Phys.*, **2012**, *3*, 333 – 361.
10. Scholes, G.D.; Fleming, G.R.; Chen, L.X.; Aspuru-Guzik, A.; Buchleitner, A.; Coker, D.F.; Engel, G.S.; van Grondelle, R.; Ishizaki, A.; Jonas, D.M.; Lundeen, J.S.; McCusker, J.K.; Mukamel, S.; Ogilvie, J.P.; Olaya-Castro, A.; Ratner, M.A.; Spano, F.C.; Whaley, K.B.; Zhu, X. Using coherence to enhance function in chemical and biophysical systems. *Nature*, **2017**, *543*, 647 – 656.
11. Meneghin, E.; Volpato, A.; Cupellini, L.; Bolzonello, L.; Jurinovich, S.; Mascoli, V.; Carbonera, D.; Mennucci, B.; Collini, E. Coherence in carotenoid-to-chlorophyll energy transfer. *Nature Comm.*, **2019**, *9*, 3160.
12. Jumper, C.C.; Rafiq, S.; Wang, S.; Scholes, G.D. From coherent to vibronic light harvesting in photosynthesis. *Curr. Opin. Chem. Biol.*, **2019**, *47*, 39 – 46.
13. Wilde, M. M.; McCracken, J.M.; Mizel, A. Could light harvesting complexes exhibit non-classical effects at room temperature. *Proc. Math. Phys. Eng. Sci.*, **2010**, *466*, 1347 – 1363.
14. Briggs, J. S.; Eisfeld, A. Equivalence of quantum and classical coherence in electronic energy transfer. *Phys. Rev. E*, **2011**, *83*, 051911.
15. Miller, W. H. Perspective: Quantum or classical coherence?. *J. Chem. Phys.*, **2012**, *136* 210901.
16. Mukamel, S. Comment on “Coherence and uncertainty in nanostructured organic photovoltaics”. *J. Phys. Chem. A*, **2013**, *117*, 10563 –10564.

17. Halpin, A.; Johnson, P. J. M.; Miller, R. J. D. Comment on “Engineering coherence among excited states in synthetic heterodimer systems”, *Science*, **2014**, *344*, 1099.
18. Duan, H.-G.; Prokhorenko, V.I.; Cogdell, R.J.; Ashraf, K.; Stevens, A.L.; Thorwart, M.; Miller, R.J.D. Nature does not rely on long-lived electronic quantum coherence for photosynthetic energy transfer. *Proc. Natl. Acad. Sci. U. S. A.*, **2017**, *114*, 8493 – 8498.
19. Thyryhaug, E.; Tempelaar, R.; Alcocer, M.J.P; Židek, K.; Bina, D.; Knoester, J.; Jansen, T.L.C.; Zigmantas, D. Identification and characterization of diverse coherences in the Fenna-Matthews-Olson complex. *Nature Chem.*, **2018**, *10*, 780 – 786.
20. Olaya-Castro, A.; Lee, C.F.; Olsen, F.F.; Johnson, N.F. Efficiency of energy transfer in a light-harvesting system under quantum coherence. *Phys. Rev. B*, **2008**, *78*, 085115.
21. Lloyd, S. Quantum coherence in biological systems. *J. Phys.: Conf. Series*, **2011**, *302*, 012037.
22. Streltsov, A.; Adesso, G.; Plenio, M. B. Colloquium: Quantum coherence as a resource. *Rev. Mod. Phys.*, **2017**, *89*, 041003.
23. Mukamel, S. *Principles of Nonlinear Optical Spectroscopy*; Oxford University Press: New York, 1995.
24. Jonas, D. M. Two-dimensional Femtosecond Spectroscopy. *Ann. Rev. Phys. Chem.*, **2003**, *54*, 425 – 463.
25. Streltsov, A.; Singh, U.; Dhar, H.S.; Bera, M.N.; Adesso, G. Measuring Quantum Coherence with Entanglement. *Phys. Rev. Lett.*, **2015**, *115*, 020403.
26. Mabuchi, H.; Doherty, A. C. Cavity Quantum Electrodynamics: Coherence in Context. *Science*, **2002**, *298*, 1372 – 1377.
27. May, V.; Kühn, O. *Charge and Energy Transfer Dynamics in Molecular Systems*; Weinheim: Wiley-VCH, 2011.

28. McLone, R. R.; Power, E. A. On the interaction between two identical neutral dipole systems, one in the excited state and the other in the ground state. *Mathematika* **1964**, *11*, 91 – 94.
29. Avery, J. S. Resonance energy transfer and spontaneous photon emission. *Proc. Phys. Soc.* **1966**, *88*, 1 – 8.
30. Power, E. A.; Thirunamachandran, T. Quantum electrodynamics with non-relativistic sources. III. Intermolecular interactions. *Phys. Rev. A* **1983**, *28*, 2671 – 2675.
31. Andrews, D. L. A Unified theory of radiative and radiationless molecular energy transfer. *Chem. Phys.* **1989**, *135*, 195 – 210.
32. Salam, A. The unified theory of resonance energy transfer according to molecular quantum electrodynamics. *Atoms* **2018**, *6*, 56.
33. Jones, G. A.; Bradshaw, D. S. Resonance energy transfer: From fundamental theory to recent applications. *Front. Phys.* **2019**, *7*, 100.
34. Cohen, J. L.; Berman, P. R. Amplification without inversion: Understanding probability amplitudes, quantum interference and Feynman rules in a strongly driven system. *Phys. Rev. A*, **1997**, *55*, 3900 – 3917.
35. Craig, D. P.; Thirunamachandran, T. *Molecular Quantum Electrodynamics*; Dover: New York, 1998.
36. Salam, A. *Molecular Quantum Electrodynamics*; John Wiley & Sons, Inc.: Hoboken, 2010.
37. Andrews, D. L.; Jones, G. A.; Salam, A.; Woolley, R. G. Perspective: Quantum Hamiltonians for optical interactions. *J. Chem. Phys.* **2018**, *148*, 040901.
38. Andrews, D. L.; Bradshaw, D. S. Virtual photons, dipole fields and energy transfer: A quantum electrodynamical approach. *Eur. J. Phys.*, **2004**, *25*, 845 – 858.

39. Daniels, G. J.; Jenkins, R. D.; Bradshaw, D. S.; Andrews, D. L. Resonance Energy Transfer: The Unified Theory Revisited. *J. Chem. Phys.* **2003**, *119*, 2264-2274.
40. Salam, A. Molecular quantum electrodynamics in the Heisenberg picture: A field theoretic viewpoint. *Int. Rev. Phys. Chem.* **2008**, *27*, 405 – 448.
41. Grinter, R. A.; Jones, G. A. Resonance Energy Transfer: The Unified Theory via Vector Spherical Harmonics. *J. Chem. Phys.* **2016**, *145*, 074107.
42. Agranovitch, M.; Maradudin, A. A. *Electronic Excitation Energy Transfer in Condensed Matter*; North-Holland: Amsterdam, 1982.
43. Hsu, C. P.; Fleming, G. R.; Head-Gordon, M.; Head-Gordon, T. Excitation Energy Transfer in Condensed Media. *J. Chem. Phys.* **2001**, *114*, 3065 – 3072.
44. Avanki, K. N.; Ding, W.; Schatz, G. C. Resonance Energy Transfer in Arbitrary Media: Beyond the Point Dipole Approximation. *J. Phys. Chem. C* **2018**, *122*, 29445 – 29456.
45. Craig, D. P.; Thirunamachandran, T. Third-body mediation of resonance coupling between identical molecules. *Chem. Phys.* **1989**, *135*, 37 – 48.
46. Daniels, G. J.; Andrews, D. L. The electronic influence of a third-body on resonance energy transfer. *J. Chem. Phys.* **2002**, *116*, 6701 – 6712.
47. Salam, A. Mediation of resonance energy transfer by a third molecule. *J. Chem. Phys.* **2012**, *136*, 014509.
48. Andrews, D. L.; Ford, J. S. Resonance energy transfer: Influence of neighbouring matter absorbing in the wavelength region of the acceptor. *J. Chem. Phys.* **2013**, *139*, 014107.
49. Caprasecca, S.; Curutchet, C.; Menucci, B. Toward a unified modelling of environment and bridge-mediated contributions to electronic energy transfer: A fully polarisable QM/MM/PCM approach. *J. Chem. Theory Comput.* **2012**, *8*, 4462 – 4473.



50. Caprasecca, S.; Menucci, B. Excitation energy transfer in donor-bridge-acceptor systems: A combined quantum-mechanical/classical analysis of the role of the bridge and the solvent. *J. Phys. Chem. A* **2014**, *118*, 6484 – 6491.
51. Weeraddana, D.; Premaratne, M.; Andrews, D. L. Direct and third-body mediated resonance energy transfer in dimensionally constrained nanostructures. *Phys. Rev. B* **2015**, *92*, 035128.
52. Weeraddana, D.; Premaratne, M.; Andrews, D. L. Quantum electrodynamics of resonance energy transfer in nanowire systems. *Phys. Rev. B* **2016**, *93*, 075151.
53. Andrews, D. L.; Forbes, K. A. Quantum features in the orthogonality of optical modes for structured and plane-wave light. *Opt. Lett.*, **2018**, *43*, 3249 – 3252.
54. Juzeliunas, G.; Andrews, D. L. Quantum electrodynamics of resonant energy transfer in condensed matter. *Phys. Rev. B* **1994**, *49*, 8751 – 8763.
55. Juzeliunas, G.; Andrews, D. L. Quantum electrodynamics of resonance energy transfer. *Adv. Chem. Phys.* **2000**, *112*, 357 – 410.
56. Lock, M. P. E.; Andrews, D. L.; Jones, G. A. On the nature of long-range electronic coupling in a medium: Distance and orientational dependence for chromophores in molecular aggregates. *J. Chem. Phys.* **2014**, *140*, 044103.
57. Gardiner, C. W.; Zoller, P., *Quantum Noise: A Handbook of Markovian and Non-Markovian Quantum Stochastic Methods with Applications to Quantum Optics*; Springer: Heidelberg, 2010.
58. Nielsen, M. A.; Chuang, I. L. *Quantum Computing and Quantum Information, 10<sup>th</sup> Anniversary Edition*; Cambridge University Press: Cambridge, 2010.
59. Breuer, H. –P.; Petruccione, F., *The Theory of Open Quantum Systems*; Oxford University Press: Oxford, 2006.

60. Moiseyev, N., *Non-Hermitian Quantum Mechanics*, Cambridge University Press: Cambridge, 2011.

61. Scholes, G. D. Coherence from Light Harvesting to Chemistry, *J. Phys. Chem. Lett.* **2018**, *9*, 1568 – 1572.